Temperature dependence of the second-order susceptibility in calamitic ferroelectric liquid crystals

N. Pereda; C. L. Folcia; J. Etxebarria; J. Ortega; M. B. Ros

PLEASE SCROLL DOWN FOR ARTICLE

Temperature dependence of the second-order susceptibility in calamitic ferroelectric liquid crystals

by N. PEREDA, C. L. FOLCIA, J. ETXEBARRIA*

Departamento de Física de la Materia Condensada, Facultad de Ciencias,
Universidad de País Vasco, Apdo. 644, 48080 Bilbao, Spain

J. ORTEGA

Departamento de Física Aplicada II, Facultad de Ciencias,
Universidad de País Vasco, Apdo. 644, 48080 Bilbao, Spain

and M. B. ROS

Departamento de Química Orgánica, Facultad de Ciencias,
Universidad de Zaragoza, 50009 Zaragoza, Spain

The d_{ij} coefficients of the second-order susceptibility tensor for second harmonic generation were detemined for a calamitic ferroelectric liquid crystal (FLC) specifically designed for applications in non-linear optics. The measurements were performed at different temperatures in the SmC* phase. In accordance with the design methodology of these materials, the coefficient along the polar axis d_{22} is the greatest, and depicts an expected behaviour in the whole range of the ferroelectric phase. On the other hand, the temperature dependence of d_{21}, d_{23}, and d_{25}, is anomalous to some extent, including a sign inversion of d_{23} at a certain temperature. These results, which contrast with those reported recently for non-calamitic FLCs, were qualitatively interpreted in the light of different conformations which, by virtue of plausible distortions of the molecular core, could coexist in the sample.

1. Introduction

Thin films of non-linear optical (NLO) organic materials have attracted great attention due to their relevance to the fabrication of ultrafast electro-optic modulators. In particular, ferroelectric liquid crystals (FLCs) have increasingly become the subject of NLO studies because their molecular structures permit the incorporation of NLO chromophores with high hyper-polarizability [1, 2]. In addition, FLCs offer some advantages over other organic systems: self-assembly into a polar structure, suitable for showing bulk NLO properties, and easier integration with semiconductor devices than solid crystals.

The second-order NLO property most thoroughly studied in FLCs is second harmonic generation (SHG). In this process, two photons with frequency ω combine to give one photon with frequency 2ω. The power of the light at 2ω, $P^{2\omega}$ can be written as $P^{2\omega} \propto d_{\text{eff}}^2 (P^\omega)^2$, where P^ω is the power of the incident beam and d_{eff} is a linear combination of the second-order susceptibility tensor

coefficients d_{ijk}, whose specific form depends on the experimental conditions. Thus, a complete characterization of the SHG properties of a particular material requires the determination of the whole **d** tensor. In the case of a SmC* phase, this tensor contains four independent coefficients provided that the material is non-absorbing and, therefore, Kleinman conditions are valid.

In the last few years, some progress has been achieved in the design of new FLCs with enhanced SHG. However, in comparison with this synthesis effort, very few materials have been fully characterized. Up to now, most SHG studies have been limited to a mere evaluation of d_{eff} at the phase matching condition and at a particular temperature. Although usually this is considered enough to get a first insight of the SHG capabilities of the material, it is also clear that some other important features are missed in such a restricted investigation. For example, the coefficient of the **d** tensor along the polar direction (d_{222}), which is usually optimized in the synthesis process [1, 2], does not contribute to the SHG at the phase matching configuration. The reason for the lack of complete SHG

*Author for correspondence.

data is the rather indirect way in which the individual d_{ijk} coefficients are deduced from the raw measurements which, on the other hand, should have enough quality to permit a reliable data process.

Another interesting point which has received scarce attention in the literature, concerns the d_{ijk} temperature dependence in the SmC* phase. In this sense, it is to be expected that the behaviour of the different d_{ijk} coefficients with temperature, and their relation with other spontaneous quantities like polarization or tilt angle, could provide information about microscopic aspects involved in the non-linear response. In a previous work we presented the first results on the d_{ijk} temperature dependence for a non-calamitic metallorganic FLC [3]. The behaviour of the different d_{ijk} coefficients was interpreted in terms of some simple molecular aspects. In this respect it seems of interest to carry out a similar investigation on different materials.

In this paper we present measurements of the temperature dependence of the whole **d** tensor in the SmC* phase of a calamitic compound (W316) especially designed for NLO applications by Walba *et al.* [1, 2]. The molecular structure together with the phase sequence are shown in figure 1. The material belongs to a series of FLCs which can now be considered classical in the NLO field. The acceptor–donor array is the *o*-nitroalkoxy system, which is also responsible for the main part of the transverse dipole moment. The material has a high spontaneous polarization, with a maximum $\mathbf{P}_s = 350\,\mathrm{nC\,cm}^{-2}$ [1, 4].

2. Experimental

SHG measurements were carried out using a standard technique [5] (figure 2). The fundamental light came from a Q-switched Nd:YAG laser (wavelength $\lambda = 1064\,\mathrm{nm}$ and pulse width 6 ns). The peak intensity at the sample position was $0.8\,\mathrm{MW\,cm}^{-2}$. The second harmonic light was separated from the fundamental beam after passing through an IR cut filter, a green glass filter and an interference filter, and was detected using a photomultiplier. The second harmonic light generated by a LiNbO$_3$ crystal was detected with another photo-
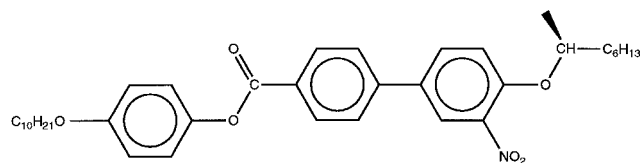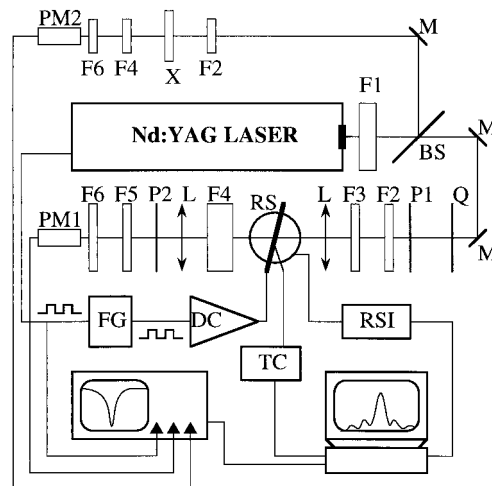

Figure 2.   Experimental set-up for SHG measurements: F1 (neutral density filter), F2 (VIS cut filter), F3 (IR interference filter), F4 (IR cut filters), F5 (green glass filter), F6 (interference filter for second harmonic light), BS (beam splitter), M (mirrors), Q (quarter wave plate), P1 (polarizer), P2 (analyser), L (lenses), X (LiNbO$_3$ crystal), RS (rotating stage), PM1 (main signal photomultiplier), PM2 (reference photomultiplier), FG (function generator), DC (amplifier), TC (temperature controller), RSI (rotating stage interface).

multiplier in the reference branch to compensate for intensity fluctuations and laser pulse spreading with time.

The liquid crystal material was homeotropically aligned in a glass cell treated with hexadecyltrimethyl-ammonium bromide (HTAB). The sample thickness was $58\,\mu\mathrm{m}$ and the cell gap was maintained with two aluminium spacers which were also used as electrodes. Good alignment was obtained in the SmC* phase by cooling the sample from the isotropic phase at a rate of $0.1^{\circ}\mathrm{C\,min}^{-1}$. An electric field of $250\,\mathrm{V\,mm}^{-1}$ was used to unwind the helicoidal arrangement characteristic of the SmC* phase. To avoid damaging the sample, a square wave was used instead of a continuous one. The laser pulse triggered the oscilloscope and was synchronized with the electric wave to permit a complete helix unwinding at each period. Prior to the measurements, a check was made, using polarizing microscopy, that electric field frequencies up to 10 Hz were low enough to allow for a complete switching of the molecules.

In performing the experiments, we noticed that the ratio between the second harmonic generated by the sample and the LiNbO$_3$ crystal at the reference branch was not independent of the light intensity (as it should be) for high light powers and pulse frequencies. It was checked that the second harmonic light from the LiNbO$_3$ crystal behaved normally, being independent of the laser pulse frequency and showing a quadratic dependence on

W316   Cr 30°C SmC* 56°C SmA 94°C I

Figure 1.   Chemical structure and phase sequence on cooling for W316.

the incident light power. Therefore, the origin of this anomalous phenomenon was attributed to a strong heating of the sample due to the high irradiation in the main branch of the equipment. On lowering the laser pulse frequency or light intensity, and therefore the irradiation, the effect became less pronounced as a consequence of a better heat dissipation in the sample. For intensities of $0.8\,\mathrm{MW\,cm^{-2}}$ and at frequencies below $3\,\mathrm{Hz}$ the effect was negligible. Therefore the laser pulse frequency selected for the measurements was $3\,\mathrm{Hz}$.

3. Results

SmC* phases are characterized by the point group 2 with the spontaneous polarization $\mathbf{P}_s$ along the two fold axis. Therefore, the contracted $\mathbf{d}$ tensor which describes the SHG process in these systems is:

$$(d_{ij}) = \begin{pmatrix} 0 & 0 & 0 & d_{14} & 0 & d_{16} \\ d_{21} & d_{22} & d_{23} & 0 & d_{25} & 0 \\ 0 & 0 & 0 & d_{34} & 0 & d_{36} \end{pmatrix} \quad (1)$$

where the number of independent d_{ij} coefficients is reduced to four $(d_{25} = d_{36} = d_{14},\ d_{23} = d_{34},\ d_{21} = d_{16})$ assuming Kleinman conditions to be valid. The d_{ij} tensor is referred to a coordinate system in which z is along the optic axis and y is parallel to $\mathbf{P}_s$.

The second harmonic power for ee-o or oo-o configurations (see figure 3) can be approximated by the following expression [6, 7]:

$$P^{2\omega} = \frac{8\omega^2 d_{\mathrm{eff}}^2 L^2 (t^\omega)^4 (t^{2\omega})}{\varepsilon_0 c^3 (n_{\mathrm{e,o}}^\omega)^2 n_\mathrm{o}^{2\omega} A} \left[\frac{\sin\left(\dfrac{\Delta k L}{2}\right)}{\left(\dfrac{\Delta k L}{2}\right)} \right]^2 (P^\omega)^2 \quad (2)$$

where L is the interaction length, t^ω and $t^{2\omega}$ are standard Fresnel transmission factors, A is the beam area and P^ω the power of the incident light; $n_\mathrm{o}^{2\omega}$ and $n_{\mathrm{e,o}}^\omega$ are the refractive indices corresponding to the second harmonic and fundamental light, respectively.

When the fundamental light is polarized parallel to $\mathbf{P}_s$ (o-ray), we have $\Delta k = 4\pi/\lambda(n_\mathrm{o}^{2\omega} - n_\mathrm{o}^\omega)$ and $d_{\mathrm{eff}} = d_{22}$. In this configuration Δk is constant and Maker fringe profiles like those represented in figure 4 were obtained. Absolute values of d_{22} were directly determined from the maxima of the curves. A y-cut quartz sample $(d_{11} = 0.4\,\mathrm{pm\,V})$ was used as a standard for calibration purposes.

When the incident light is polarized perpendicularly to $\mathbf{P}_s$ (e-ray), we have $\Delta k = 4\pi/\lambda[n_\mathrm{o}^{2\omega} - n_\mathrm{e}^\omega(\theta - \theta_\mathrm{t})]$ and expression (1) yields

$$d_{\mathrm{eff}} = d_{21}\cos^2(\theta - \theta_\mathrm{t}) + d_{23}\sin^2(\theta - \theta_\mathrm{t})$$
$$+ 2d_{25}\sin(\theta - \theta_\mathrm{t})\cos(\theta - \theta_\mathrm{t}) \quad (3)$$

θ being the refraction angle (calculated assuming an average refractive index of 1.6) and θ_t the optical tilt
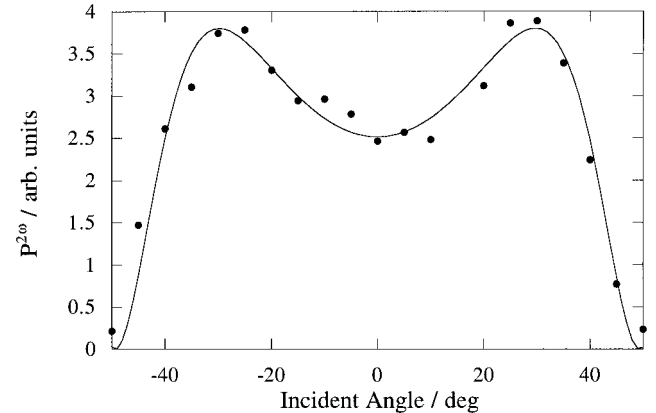

Figure 4. Second harmonic intensity (in arbitrary units) versus incident angle in oo-o field configuration. The data correspond to $T = 46°\mathrm{C}$. Maker fringes can be clearly observed; from the maxima of these fringes the d_{22} coefficient was extracted. The continuous line is only an eye-guide.
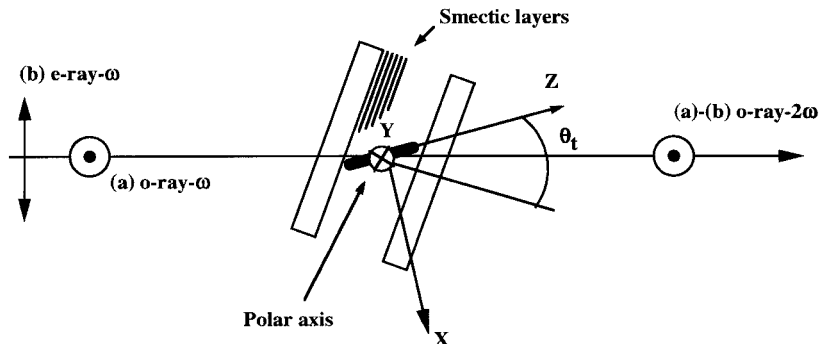

Figure 3. Experimental geometry for SHG measurements. The electric field is applied along the polar axis (Y) which is also the rotation axis of the sample. (a) oo-o field geometry: from this configuration the d_{22} coefficient can be obtained. (b) ee-o field geometry: from this configuration d_{21}, d_{23} and d_{25} can be extracted.

angle. Therefore, Δk depends on θ in this configuration, and phase matching occurs if $\Delta k = 0$ for a given θ. A typical $P^{2\omega}$ versus incident angle plot is represented in figure 5. Besides the phase matching peak a certain number of secondary maxima can be observed.

In this experimental geometry, it is much more difficult to extract the individual d_{ij} coefficients from the measurements. This was accomplished following the procedure described in previous work [3]. The $d_{eff}(\theta)$ values were determined at the maxima of the $P^{2\omega}$ curve (figure 5) where ΔkL values are known. Then, d_{21}, d_{23} and d_{25} were deduced by fitting the $d_{eff}(\theta)$ points to equation (3). The tilt angle was not considered as a free parameter for these fits, but its value was taken from independent measurements performed on a planar sample. Several fitting schemes with a different number of fit parameters in equation (3) were used. Obviously the best fits were obtained with three free parameters, but the results with two unknowns (the third one deduced from d_{eff} at phase matching or d_{eff} at $\theta = \theta_t$) were also considered.

The d_{ij} coefficients were obtained at different temperatures in the SmC* phase. The results are represented in figure 6. Error bars in this figure were estimated by taking into account the values derived from the different fits and including possible errors in the measurements of θ_t and $P^{2\omega}$.

On the other hand, the birefringence $\Delta n = n_e^\omega - n_o^\omega$ and the dispersion $\Delta n_d = n_o^{2\omega} - n_o^\omega$ were deduced from a fit of Δk at the angular positions of the maxima and minima of the phase matching curve. The results are plotted in figure 7.

For the sake of completeness, we also give (figure 8) the d_{eff} values versus temperature at phase matching. Good agreement can be observed between the data
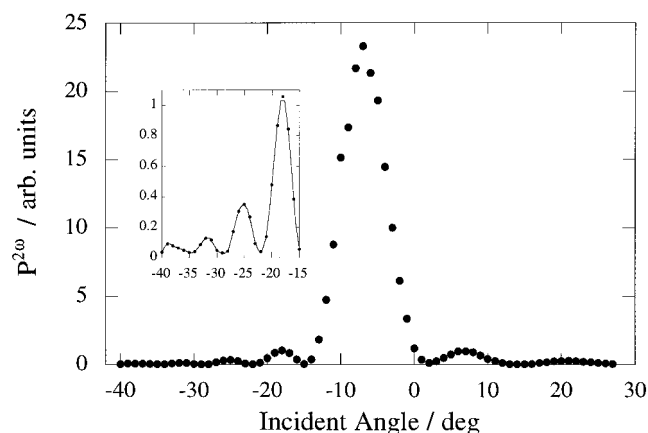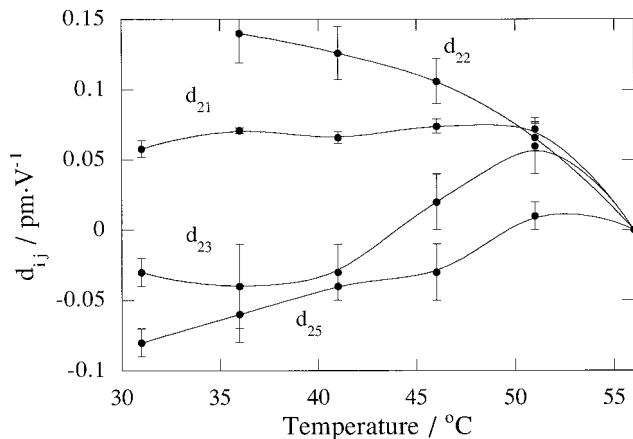

Figure 6. Temperature dependence of the individual d_{ij} coefficients in the SmC* phase. d_{22} was determined from the maxima of Maker fringes in the oo-o configuration and the rest of the coefficients were deduced from measurements in the ee-o configuration. The continuous lines have been drawn only for eye-guides.
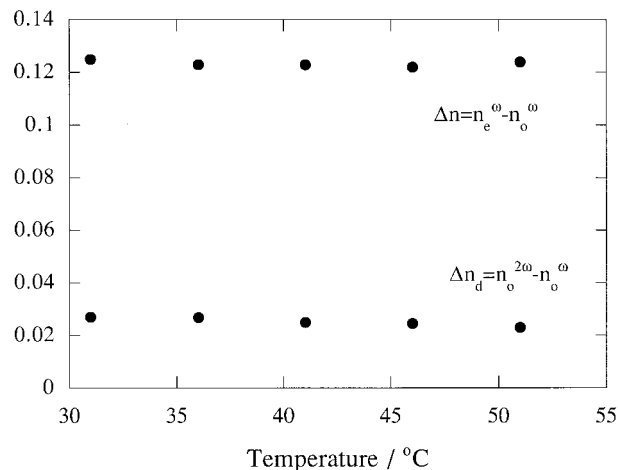

Figure 7. Birefringence $\Delta n = n_e^\omega - n_o^\omega$ and dispersion $\Delta n_d = n_o^{2\omega} - n_o^\omega$ in the SmC* phase of W316 calculated from the positions of the maxima and minima in the phase matching curves.

deduced from the d_{ij} coefficients and those measured directly. The magnitude of d_{eff} lies between those of W313 [8] and W314 [9]. This is to be expected since their molecular cores are quite similar and also include the *o*-nitroalkoxy unit as a donor–acceptor array.

4. Discussion

As can be seen in figure 6, d_{22} is greater than the other coefficients over the whole ferroelectric phase of W316. This is in accordance with the design methodology of this type of material, which intrinsically favours the non-linear response connected with d_{22}. Moreover, this coefficient depicts the typical trend of any quantity coupled to the polar order in the SmC* phase. In this
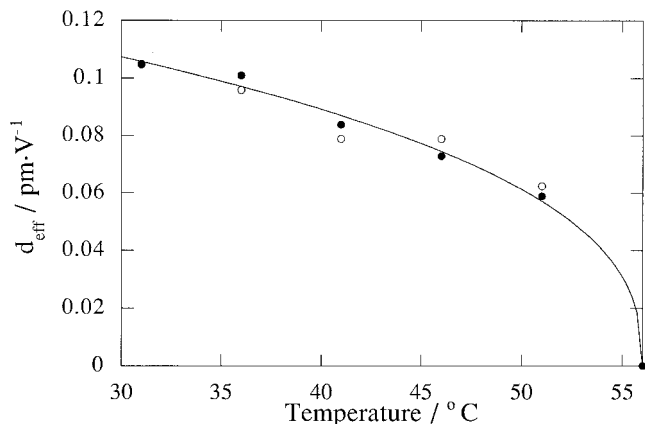

Figure 5. Second harmonic intensity (in arbitrary units) as a function of the angle of incidence at $T = 36°C$. The absolute maximum of the curve corresponds to the phase matching condition; secondary maxima can also be observed.

Figure 8. Temperature dependence of d_{eff} at phase matching. Open circles correspond to values obtained from the d_{ij} data and full circles to direct measurements of the intensity of the phase matching peak. The continuous line is only an eye-guide.

sense, the temperature dependence of d_{22} resembles that of the tilt angle and the spontaneous polarization [1, 4]. This is not the case for the other d_{ij} coefficients. In fact, d_{21} is constant within error and d_{23} and d_{25} present an anomalous behaviour which includes a clear sign inversion in the case of d_{23} at a given temperature in the SmC* phase. It is worth mentioning that this temperature behaviour was reproduced on another sample, which gives us some confidence in the results.

The results can be qualitatively interpreted in the light of some general aspects of the molecular structure. According to Walba *et al.* [1, 2], the *o*-nitroalkoxy-benzene unit in W316 type compounds is responsible for the main contribution to the transverse molecular dipole moment $\mu_\perp$. In this sense, the spontaneous polarization $\mathbf{P}_s$ is a consequence of the degree of orientation of these active units along the polar direction. This conjugated system can also be considered to account for the non-linear response when the excitation field is along $\mu_\perp$, and is therefore the origin of d_{22}. Consequently, according to this simple scheme $\mathbf{P}_s$ and d_{22} will depend on the characteristics and orientation of the same molecular unit. Thus it seems reasonable to conclude that both quantities will present a similar dependence on the degree of order and therefore on temperature. On the other hand, d_{21}, d_{23}, and d_{25} require the contribution from non-diagonal coefficients of the second order hyperpolarizability tensor β. These coefficients cannot be accounted for by a simple one-dimensional model, but will depend on the molecular structure in a more complicated manner.

In a first approximation, a rigid molecular model can be proposed to explain the results shown in figure 6. If we consider the simplest case of a rigid molecule in which only rotations of the core around the molecular

direction (z' axis) are allowed (figure 9), then the components b_{IJK} of the mean hyperpolarizability tensor per molecule [10] result:

$$b_{YZZ} = \langle \cos \psi \rangle \beta_{y'z'z'} \tag{4a}$$

$$b_{YXX} = \langle \cos^3 \psi - 2 \sin^2 \psi \cos \psi \rangle \beta_{y'x'x'} + \langle \cos \psi \sin^2 \psi \rangle \beta_{y'y'y'} \tag{4b}$$

$$b_{YXZ} = \langle \cos 2\psi \rangle \beta_{y'x'z'} \tag{4c}$$

$$b_{YYY} = \langle \cos^3 \psi \rangle \beta_{y'y'y'} + \langle 3 \cos \psi \sin^2 \psi \rangle \beta_{y'x'x'} \tag{4d}$$

where ψ is the angle between y' (parallel to $\mu_\perp$) and Y (parallel to $\mathbf{P}_s$), and Z (which we assume parallel to z') stands for the optic axis direction. It is evident that expressions $(4a)$–$(4d)$ are not consistent with the behaviour depicted in figure 6 for the d_{ij} coefficients. In particular, according to $(4a)$, d_{23} (which is proportional to b_{YZZ}) should depend on temperature similarly to $\mathbf{P}_s$, since [11]:

$$\mathbf{P}_s \approx N\mu_\perp \langle \cos \psi \rangle \tag{5}$$

N being the molecular density. On the other hand, it is not obvious that expressions $(4b)$ and $(4c)$ can reproduce the behaviour observed for d_{25} (which derives from b_{YXZ}) or d_{21} (proportional to b_{YXX}). Finally, it is to be pointed out that these conclusions are not substantially modified when the model is generalized by considering other (much more restricted) degrees of freedom of the rigid core.

From the above analysis it is clear that a rigid molecular model must be discarded for W316, and molecular deformations should be taken into account. Furthermore, it seems likely that these molecular distortions do not affect d_{22} and $\mathbf{P}_s$, but can however alter drastically the non-diagonal components of β. In this situation, the anomalous behaviour of d_{21}, d_{23}, and d_{25} would be a consequence of the great variety of conformations that, in virtue of the characteristic flexibility of a calamitic structure, are present in the bulk [12]. This alternative model is analogous to that proposed for some FLCs where the coexistence of different conformers, with a temperature dependent probability, can
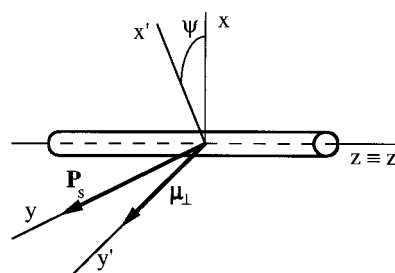

Figure 9. Schematic diagram showing the laboratory (x, y, z) and molecular (x', y', z') coordinate systems.

produce an inversion of the polarization in the ferro-electric phase [13]. In this context, the hypothesis can be proposed that sign inversion of some d_{ij} coefficients would not be unusual in FLCs (especially for d_{23} and d_{25}, where there is no contribution from $\beta_{y'y'y'}$). Evidently, further investigations are necessary to confirm this point.

In the case of the metallorganic series of FLCs studied in ref. [3], d_{21}, d_{23}, and d_{25} depict the normally expected temperature dependence, analogous to d_{22} in figure 6, in agreement with the rigid molecular scheme [3]. These non-calamitic mesogens consist of a planar central core that constitutes the conjugated system, and four organic chains joined to it. In this situation it can be assumed that, contrary to calamitic FLCs, the planar core behaves as a rigid structure, and therefore the contribution of each molecule to the second-order susceptibilty of the bulk depends mainly on its orientation. Thus the d_{ij} components presented in ref. [3] could be described by expressions (4 a)–(4 d). In fact, the d_{23} coefficient, which turned out to be greater than the others, resembles the P_s temperature dependence in agreement with (4 a).

In summary, the second-order susceptibility tensor has been completely characterized for the calamitic FLC W316 at different temperatures in the SmC* phase. The d_{ij} coefficients were compared with those of non-conventional mesogens like metallorganic FLCs. The anomalous trend of the non-diagonal d_{ij} coefficients in W316 was interpreted as a consequence of the non-rigid character of its molecular core, and is expected to occur in other rod-like compounds. This fact clearly prevents a straightforward interpretation of the relative size of the d_{ij} coefficients on a microscopic scale, as was carried out in ref. [3] for an *ortho*-platinated β-diketonate complex. Investigations to clarify this point, as well as the determination of the d_{ij} tensor in other calamitic compounds under different conditions, are being carried out.

References

[1] WALBA, D. M., ROS, M. B., CLARK, N. A., SHAO, R., JOHNSON, K. M., ROBINSON, M. G., LIU, J. Y., and DOROSKI, D. J., 1991, *Mol. Cryst. liq. Cryst.*, **198**, 51.

[2] WALBA, D. M., ROS, M. B., SIERRA, T., REGO, J. A., CLARK, N. A., SHAO, R., WAND, M. D., VOHRA, R. T., ARNETT, K. E., and VELSCO, S. P., 1991, *Ferroelectrics*, **121**, 247.

[3] ORTEGA, J., FOLCIA, C. L., ETXEBARRIA, J., ROS, M. B., and MIGUEL, J. A., 1997, *Liq. Cryst.*, **23**, 285.

[4] HERMANN, D. S., KOMITOV, L., LAGERWALL, S. T., ANDERSON, G., SHASHIDAR, R., SELINGER, J. V., and GIEẞELMANN, F., 1996, *Ferroelectrics*, **181**, 371.

[5] TAGUCHI, A., OUCHI, Y., TAKEZOE, H., and FUKUDA, A., 1989, *Jpn. J. appl. Phys.*, **28**, L 997.

[6] YARIV, A., and YEH, P., 1984, *Optical Waves in Crystals* (John Wiley & Sons).

[7] HERMAN, W. N., and HAYDEN, L. M., 1995, *J. opt. Soc. Am. B*, **12**, 416.

[8] ORTEGA, J., FOLCIA, C. L., ETXEBARRIA, J., ARTAL, M. C., ROS, M. B., and SERRANO, J. L., 1996, *Adv. Mater.*, **8**, 411.

[9] LIU, J. Y., ROBINSON, M. G., JOHNSON, K. M., WALBA, D. M., ROS, M. B., CLARK, N. A., SHAO, R., and DOROSKI, D., 1991, *J. appl. Phys.*, **70**, 3426.

[10] OUDAR, J. L., and ZYSS, J., 1982, *Phys. Rev. A*, **26**, 2016.

[11] STEGEMEYER, H., MEISTER, R., HOFFMANN, U., and KUCZYNSKI, W., 1991, *Liq. Cryst.*, **10**, 295.

[12] GLASER, M. A., GINZBURG, V. V., CLARK, N. A., GARCÍA, E., WALBA, D. M., and MALZBENDER, R., 1995, *Mol. Phys. Rep.*, **10**, 26.

[13] PATEL, J. S., and GOODBY, 1987, *Opt. Eng.*, **26**, 373.